Desalination and Water Treatment
www.deswater.com
doi: 10.1080/19443994.2016.1160438

57 (2016) 26089–26100
November

Taylor & Francis
Taylor & Francis Group

Synthetic zeolite from coal bottom ash and its application in cadmium and nickel removal from acidic wastewater

Haixia Wang[a,b,*], Xiuru Wang[a,*], Zhenghe Xu[b], Mingliang Zhang[b]

[a]*School of Soil and Water Conservation, Beijing Forestry University, Beijing 100083, China, Tel. +86 1062338044; emails: stu_wanghx@126.com (H. Wang), wang-xr@163.com (X. Wang)*
[b]*School of Resources and Environment, University of Jinan, Jinan 250022, China, Tel. +86 53182769233; emails: stu_xuzh@ujn.edu.cn (Z. Xu), stu_zhangml@ujn.edu.cn (M. Zhang)*

Received 8 October 2015; Accepted 26 February 2016

ABSTRACT

The adsorption properties of synthetic zeolite from coal bottom ash (CBA) were investigated for Cd and Ni removal from simulated acidic wastewater. The results showed that alkaline fusion synthetic zeolite significantly increased the specific surface area, pore volume, and cation exchange capacity (CEC) compared with CBA. The effects of various experimental parameters such as coexisting ion competition, pH, contact time, and temperature on the adsorption capacity and adsorption mechanism were investigated. Compared with single-metal ion adsorption, the adsorption capacity for Cd or Ni decreased in multiple-metal ions adsorption due to the competition effect of coexisting ion. Adsorption efficiency increased with increasing pH and the equilibrium was achieved at around 5.5 (>pH_{pzc} 4.5). The adsorption equilibrium was achieved within 4 h and followed the pseudo-second-order kinetic model. The result concluded that ion exchange was the primary adsorption mechanism. Moreover, zeolite exhibited strong neutralizing capacity, which could be attractive for acidic wastewater treatment.

Keywords: Zeolite; Coal bottom ash; Adsorption isotherm; Ion exchange

1. Introduction

Heavy metals have been considered as one kind of the most harmful contaminants because of their non-biodegradability and high accumulation [1]. Consequently, the removal of heavy metals from wastewater has become a major concern in recent decades [2]. Among metal treatment methods, the adsorption by suitable materials has been considered as an effective method for heavy metals removal from wastewater [3]. There will be still a growing demand to develop new low-cost and efficient adsorbents for heavy metals removal from wastewater, particularly if the adsorbents are waste materials [4].

Coal ash (fly ash and bottom ash) is one kind of solid waste generated from coal burning power plants. Enormous amounts of coal ash are generated worldwide in annual basis. For instance, in China, the amount exceeded 400 million tons in 2010. The improper disposal of the large amounts of coal ash can cause environmental pollution, and it has become a heavy burden to the coal mining sector [5]. In recent years, efforts have been made to recycle coal ash, but less than half amount of coal ash has been used for

---

*Corresponding authors.

concrete production, embankments and other structural fills, waste solidification, road base stabilization, and mine reclamation [6]. Therefore, more effort should be put into the recycle and reuse of coal ash. At present, coal ash has been reported as a potential adsorbent for the treatment of wastewater containing heavy metals or organic compounds [7]. Much work on heavy metal adsorption by coal ash has been reported in recent years, but its relatively low adsorption capacity limited the application [8–10].

Conversion coal ash into zeolite is one of the attractive alternatives for recycling coal ash as it usually contains high contents of silica and alumina which are the basic elements for the formation of zeolite [11]. Converting coal ash into zeolite not only alleviates the disposal problem, but also turns solid waste into environmental remediation material. Zeolites have been applied for contaminants adsorption, e.g. dyes, heavy metals, toxic gas, benzene, and volatile organic pollutants, due to their unique physical and chemical properties (crystallinity, thermal stability, cage structure, ion-exchange capacity, etc.) [12–17].

This study focused on the investigation of conversion coal bottom ash (CBA) into zeolite X using alkaline fusion method, the examination of adsorption characteristics and mechanism of the synthesized zeolite in the removal of metal ions from acidic solution. Taking into account that Cd and Ni are priority pollutants and widely distributed in industrial wastewater (e.g. acidic electroplating wastewater, cadmium–nickel battery wastewater, and metal smelting wastewater), thus, Cd and Ni were chosen for the adsorption experiments. The objective of this study was to establish a fundamental understanding of the adsorption behavior of Cd and Ni onto zeolite, in order to provide a basis for its practical application to the treatment of acidic wastewater containing heavy metal ions.

2. Materials and methods

2.1. Bottom ash and zeolite synthesis

CBA was collected from the bottom ash hopper in Jinjiling thermal power plant, Jinan city, Shandong province, China. Alkaline fusion method was used to convert CBA into zeolite X. The CBA sample was mixed with ground NaOH pellet at a weight ratio of 1:1.2. The homogeneous mixture was then calcined in muffle furnace at temperature (600℃) for 90 min. The fusion product was ground and transferred to a 500 mL beaker which contained deionized water. The weight ratio of fused CBA powder to water was 0.2. The mixture was stirred for 24 h until the hydrogels were homogenized. The hydrogels were transferred to polytetrafluoroethylene (PTFE)-lined stainless steel autoclave and heated at 100℃ for 24 h. The solid product was separated from the supernatant by centrifugation and then washed with deionized water until the solution pH decreased to 10–11 and then dried overnight at 110℃ [18].

2.2. Physical and chemical characterization

The major chemical constituents of the samples were determined by X-ray fluorescence spectroscopy (XRF, Bruker S8 tiger, Germany). The pH of CBA and zeolite was measured by pH meter (pHS-3C, Leici, China) in 1:2.5 (w/v) solid/water suspensions after equilibrium for 24 h. The mineralogical characterization was performed by powder X-ray diffraction (XRD, Bruker D8 Advance, Germany) using Cu–Ka radiation. Surface morphology observation was performed by scanning electron microscope (SEM, Quanta FEG 250, USA), and energy dispersion spectrometer (EDS, X-Max50) was used to analyze the chemical constituents of the adsorbent before and after adsorption of metal ions. Surface area was measured by using ASAP 2020 surface area and porosity analyzer (Micromeritics, USA). The samples were outgassed overnight (12 h) under nitrogen prior to adsorption measurement. Pore distributions and pore volume were calculated using the adsorption branch of the N_2 isotherms based on the Barrett–Joyner–Halenda (BJH) model. Specific surface area was calculated by the Brunauer–Emmet–Teller (BET) method. Fourier transform infrared (FTIR) spectra were recorded in the wavenumbers range of 400–4,000 cm^{-1} using FTIR spectrometer (Nicolet 380, Thermo Scientific, USA). The point of zero charge (PZC) was determined by measuring the surface charge of the samples in deionized water at various pHs using Zeta Meter electrophoresis (Malvern, UK). Cation exchange capacity (CEC) was determined using sodium acetate method according to the US-EPA method 9081 [19].

2.3. Batch adsorption experiments

Adsorption experiments were conducted in a series of 50-mL plastics bottles at temperature 18℃. Synthetic acidic wastewater was prepared with sulfate salts of Cd(II) and Ni(II) (analytical grade reagents) in deionized water, and the pH was adjusted to 2.5. In adsorption isotherm experiments, 0.5 g of adsorbent and 50 mL of metal solution with different molar concentrations were mixed in plastics bottles at temperature 18℃ for 4 h. The solution pH in adsorption experiment was adjusted to 5.5 to avoid metal precipitation (unless otherwise stated). And then the mixtures were centrifuged and filtered through 0.45-μm filter paper for metal concentration analysis. Metal concentrations were determined using an atomic absorption spectroscopy (AA-7000 model spectrometer, Shimadzu, Japan). The adsorbed amounts of metal ions were calculated by the difference between the initial and final concentrations in equilibrium solutions.

To determine the effect of pH on Cd and Ni adsorption onto zeolite, 0.5 g of sample and 50 mL of metal ions solution (0.8 mM Cd and Ni) were mixed. The solution pH was adjusted between 2 and 7. The effect of contact time was investigated under different contact times ranging from 0 to 240 min. One gram of sample was thoroughly mixed with 100 mL of metal ions solution (0.8 mM and 1.6 mM Cd + Ni) and the mixture pH was adjusted to 4.5. At required time intervals, samples were collected and filtered for metal concentration analysis. In order to determine the effect of temperature on adsorption, 0.5 g of sample and 50 mL of metal ions (0.8 mM Cd and Ni) solution were mixed in different temperatures (18 and 45℃).

2.4. Ion-exchange mechanism

Ion exchange could be one of the primary mechanisms for metal ions removal as the synthetic zeolite exhibited high CEC [8,14]. The existence of ion exchange mechanism during the adsorption of Cd and Ni onto zeolite was investigated as follows. 0.5 g zeolite was mixed with 50 mL of metal ions solution (1.6 mM Cd and Ni) at pH 5.5 for 4 h, and then the mixtures were centrifuged and filtered through 0.45-μm filter paper for Na^+ concentration analysis. As control, the release amount of Na^+ after washing successively with deionized water (pH 5.5) was also measured. The amount for net release of Na^+ due to Cd and Ni adsorption can be calculated by subtracting the amount of Na^+ released when washing with deionized water (control) to the amount of Na^+ measured in the supernatant after Cd and Ni adsorption process.

3. Results and discussion

3.1. Characterization of CBA and its synthetic zeolite X

The main chemical compositions of the CBA and zeolite by XRF are presented in Table 1. SEM observations (Fig. 1(a) and (b) of CBA shows the particles are micro-irregular. After alkaline fusion treatment, it changed into octahedral crystal shapes corresponded to zeolite X (Fig. 1(d)–(f)), which was evidenced by the XRD data. The XRD analysis (Fig. 2) suggests that quartz is the primary crystalline phase of CBA and the synthetic zeolite is of X type. Fig. 3 illustrates the relationship between zeta potential and solution pH and the results indicate that the surface of CBA and zeolite have negative charge at pH higher than 5.0 and 4.5, respectively. The typical nitrogen adsorption–desorption isotherms of the adsorbent is shown in Fig. 4. The isotherm was of type IV which was characteristic of mesoporous material according to the N_2 sorption analysis. The specific surface area and specific pore volume of the synthetic zeolite (242.04 m^2/g and 0.096 cm^3/g, respectively) were greatly larger than those of CBA (3.39 m^2/g and 0.01 cm^3/g, respectively). The pH of CBA and zeolite was 12.6 and 10.9, respectively. The CEC of the synthetic zeolite was 1.8 meq/g, which is significantly higher than 0.06 meq/g obtained from the original CBA.

Table 1
The chemical compositions and characterization of the bottom ash and zeolite

Constituent	CBA	Zeolite
SiO_2 (%)	42.95	43.06
Al_2O_3 (%)	28.53	27.07
Na_2O (%)	0.65	19.09
CaO (%)	7.55	5.57
Fe_2O_3 (%)	4.13	2.89
TiO_2 (%)	0.94	0.81
MgO (%)	0.71	0.62
K_2O (%)	1.13	0.35
SO_3 (%)	3.36	0.32
Specific surface area (m^2/g)	3.39	242.04
Pore volume (cm^3/g)	0.01	0.096
CEC (meq/g)	0.06	1.80
pH	12.6	10.9

3.2. Adsorption isotherm studies

The adsorption isotherms of zeolite for Cd and Ni are shown in Fig. 5. Equilibrium adsorption amounts increased with the increase of equilibrium concentrations. This indicated that the synthetic zeolite had strong adsorption ability and high affinity for Cd and Ni ions.

The analysis of adsorption equilibrium data for the adsorption of Cd and Ni on zeolite was conducted by the Henry, Langmuir, Freundlich, and Dubinin–Kaganer–Radushkevich (DKR) equations.

Henry model is given as follows:

$$q_e = k_h c_e \tag{1}$$

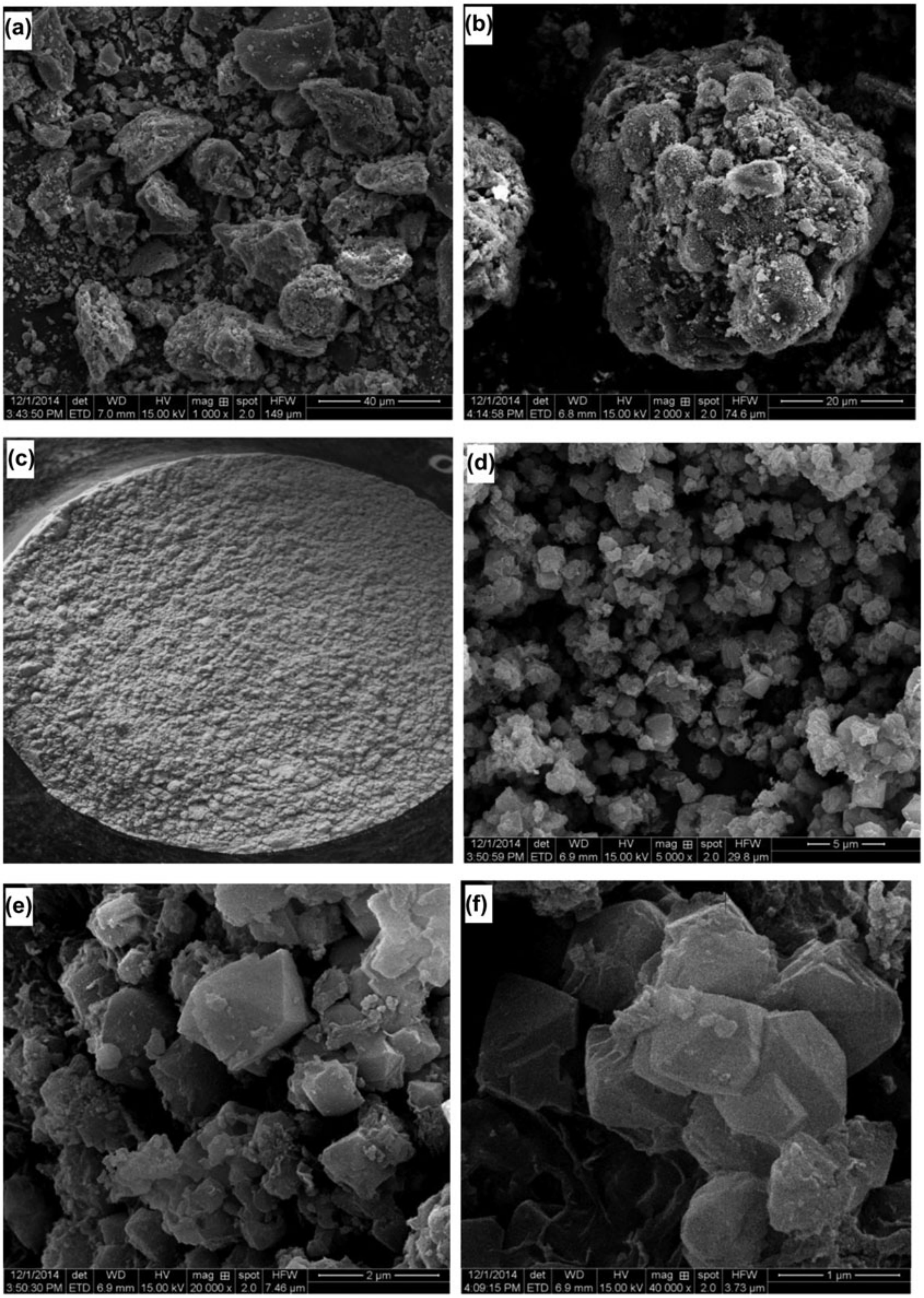

Fig. 1. SEM images of CBA (a and b); photograph of the synthetic zeolite (c); SEM images of the synthetic zeolite (d–f).

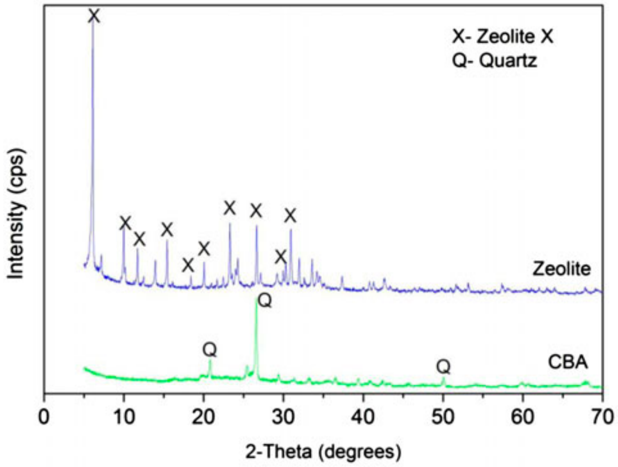

Fig. 2. XRD characteristic peaks of bottom ash and its synthetic zeolite.

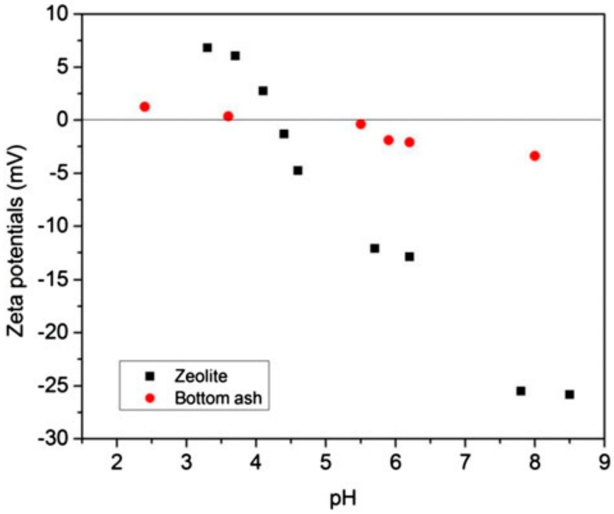

Fig. 3. Relationship between pH and surface charge of bottom ash and zeolite.

where q_e is the metal ions amount adsorbed at equilibrium (mmol/g), c_e is the equilibrium concentration of metal ions (mmol/L), k_h (mmol/g) is the Henry model constant.

The Langmuir isotherm is given as follows:

$$q_e = \frac{q_{\max} b c_e}{1 + b c_e} \tag{2}$$

where $q_{\max}$ is the maximum adsorption capacity (mmol/g) and b is the adsorption equilibrium constant (L/mmol).

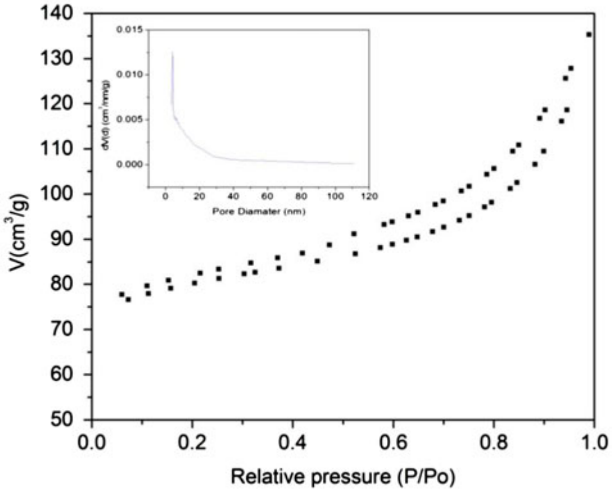

Fig. 4. N_2 adsorption–desorption isotherms and pore size distribution of zeolite.

The essential features of the Langmuir isotherm can be expressed by dimensionless constant separation factor, R_L, which can be used to predict whether an adsorption system is favorable or unfavorable [20]:

$$R_L = \frac{1}{1 + bC_o} \tag{3}$$

The value of R_L indicates the type of isotherm: unfavorable ($R_L > 1$), linear ($R_L = 1$), favorable ($0 < R_L < 1$), or irreversible ($R_L = 0$). C_o is the initial concentration of metal ions (mmol/L) [21].

The linear form of the Freundlich isotherm model is given as follows:

$$\log q_e = \log k_f + 1/n \log c_e \tag{4}$$

where k_F (mmol/g) and $1/n$ (unitless) are the Freundlich model constants related to adsorption capacity and adsorption intensity, respectively.

The DKR isotherm equation can be represented as follows:

$$\ln q_e = \ln q_m - \beta\varepsilon^2 \tag{5}$$

where q_e is the amount of adsorbed metal (mmol/g), q_m is the DKR monolayer capacity (mmol/g), β ($\mathrm{mol}^2/\mathrm{KJ}^2$) is a constant related to the sorption energy, ε is the Polanyi potential related to the equilibrium concentration through the expression:

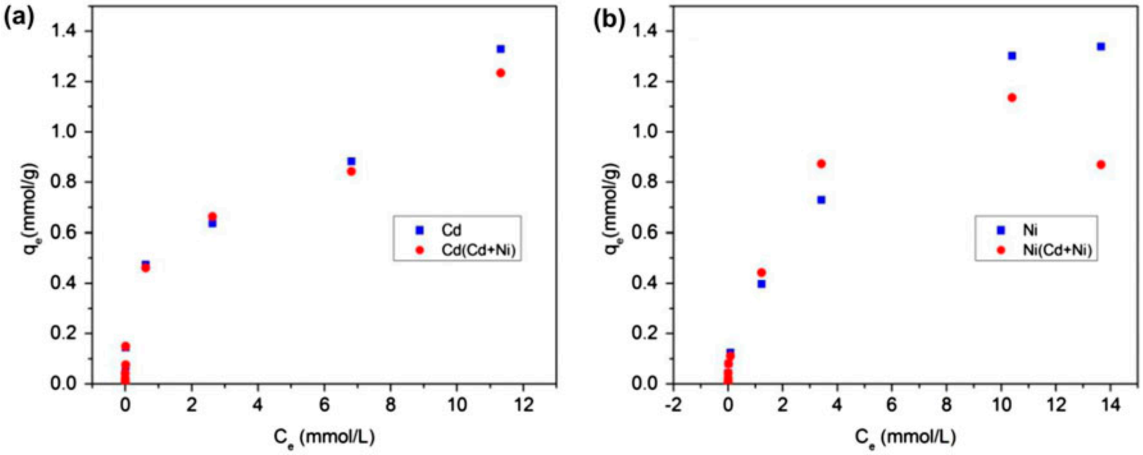

Fig. 5. The single- and multiple-metal ions adsorption capacity of (a) Cd and (b) Ni(II) on zeolite.

$$\varepsilon = RT\ln(1 + 1/c_e) \quad (6)$$

where R is the gas constant and T is the temperature (K). When $\ln q_e$ was plotted against ε^2, a straight line was obtained having a slope of β and an intercept of q_m. β is related to the sorption energy, (E), through the following relationship:

$$E = 1/\sqrt{2\beta} \quad (7)$$

The parameters of isotherm models are listed in Table 2. It shows that Cd and Ni adsorption onto zeolite was well described by the Langmuir, Freudlich, and DKR models with high R^2 values. The maximum adsorption capacities of Cd and Ni calculated by the Langmuir isotherm were 1.18 and 1.35 mmol/g, respectively. All the R_L values were between 0 and 1 indicating that the adsorption of Cd and Ni onto zeolite was favorable [22].

The effect of coexisting ion can be determined by comparison the maximum adsorption capacity of one metal ion in multi-metal ions adsorption (q^m_{max}) to that of the metal in single-metal ion adsorption (q^s_{max}) (Qin et al.; Mohan and Singh, 2002) [23]. As shown in Table 2, all the values of $q^m_{max} < q^s_{max}$ (q^s_{max} 1.18 mmol/g, q^m_{max} 1.04 mmol/g for Cd; q^s_{max} 1.35 mmol/g, q^m_{max} 0.92 mmol/g for Ni) indicated the competitive adsorption between Cd and Ni. The coexisting ion could decrease the given ion adsorption capacity onto zeolite, especially in high concentration. For example, at the initial concentration of 5 mmol/L of Cd, the adsorption capacity of Cd on zeolite was 0.475 mmol/g in Cd adsorption system and 0.461 mmol/g in Cd–Ni adsorption system.

The magnitude of E in DKR models is useful for estimating the reaction mechanism. As shown in Table 2, the E values were 10.00–12.91 kJ/mol for Cd and Ni adsorption onto zeolite. They were the orders of an ion-exchange mechanism, in which the adsorption energy lies within 8–16 kJ/mol [13]. The ion-exchange mechanism was further confirmed in the following section 3.6.

3.3. pH effect

Solution pH has a significant impact on the adsorption of heavy metals, since it determines the

Table 2
The parameters of Henry, Langmuir, Freundlich, and DKR models of the adsorption

	Langmuir			Freundlich			Henry			DKR		
Adsorption system	q_{max} (mmol/g)	b (L/mmol)	R^2	K_F (mmol/g)	$1/n$	R^2	k_h	R^2	q_{max} (mmol/g)	β (mol^2/kJ^2)	E (kJ/mol)	R^2
Cd	1.18	2.79	0.93	0.53	0.37	0.97	0.13	0.86	1.43	0.0030	12.91	0.98
Cd (Cd + Ni)	1.04	4.75	0.95	0.52	0.37	0.95	0.12	0.73	1.46	0.0031	12.70	0.98
Ni	1.35	1.41	0.95	2.47	0.56	0.95	0.11	0.91	1.89	0.0045	10.31	0.95
Ni (Cd + Ni)	0.92	2.41	0.97	0.32	0.57	0.94	0.06	0.61	1.75	0.0050	10.00	0.97

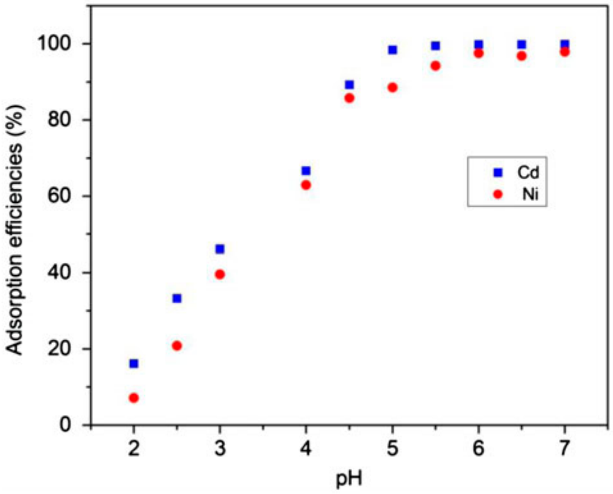

Fig. 6. Effect of pH on the adsorption of Cd and Ni (initial concentration 0.8 mM).

surface charge distribution of the synthesized zeolite, and the degree of ionization and speciation of metal ions. pH_{pzc} provides an indication of the ionization of functional groups and their potential interaction with metal species in solution [24]. At pH higher than pH_{pzc}, the zeolite surface is negatively charged and can interact with positive metal species, while at pH lower than pH_{pzc}, the zeolite surface is positively charged and can interact with negative species [25]. Fig. 6 shows the effect of solution pH on the adsorption of Cd and Ni (0.8 mM). The adsorption efficiency for Cd and Ni increased with increasing pH, and the adsorption equilibrium was achieved at pH 5.5 ($>pH_{pzc}$ 4.5), at which the removal efficiencies of Cd and Ni onto zeolite were observed to be 99.4 and 94.2%, respectively. With pH increasing, negative charges distributed on the adsorbent surface can enhance metal ions adsorption through electrostatic force of attraction. The adsorption characteristics of Cd and Ni onto zeolite showed that solution pH was the key factor affecting the adsorption characteristics. Moreover, the pH of the mixture (0.5 g of zeolite and 50 mL of acidic metal solution) was about 5.0–6.0, which showed zeolite had acid neutralizing capacity and could be attractive for acidic wastewater treatment.

3.4. Contact time effect

The effect of contact time on Cd and Ni adsorption onto zeolite is showed in Fig. 7. It showed typical biphasic kinetics with rapid adsorption during the first 15 min, followed by a slower one. Although it took slightly longer for the adsorption at high initial metal concentration (1.6 mM) to reach equilibrium than those with low initial concentration (0.8 mM), on the whole the adsorption reached equilibrium within 240 min. During the beginning of adsorption, a large number of vacant surface sites are available, whereas with gradual occupancy of these sites, it becomes difficult to be available due to repulsive forces between the metal ions on solid surface and in the bulk phase. Besides, the driving force of mass transfer between bulk liquid phase and the solid phase decreases with the passage of time, which also results in the slowing down of the adsorption during the later phase of adsorption [26].

The results of the adsorption kinetics were evaluated with pseudo-first-order and pseudo-second-order and Bangham models.

Pseudo-first-order equation:

$$\log(q_e - q_t) = \log q_e - \frac{k_1 t}{2.303} \tag{8}$$

Pseudo-second-order equation:

$$\frac{t}{q_t} = \frac{1}{k_2 q_e^2} + \frac{1}{q_e} t \tag{9}$$

where q_t is the amount of metal adsorbed (mmol/g) at time t; k_1 (1/min) and k_2 (g/mmol h) are the rate constants of the pseudo-first-order and pseudo-second-order models, respectively; t is the adsorption time (min).

Bangham equation:

$$\log q_t = \log k + \left(\frac{1}{m}\right) \log t \tag{10}$$

where q_t (mmol/g) is the adsorbed amount of solute by adsorbent at time t (min), m and k_b are the related constants.

The kinetic parameters of Cd and Ni onto zeolite are listed in Table 3. The theoretical q_e values calculated from the equation of pseudo-first-order model had great difference compared to the experimental values, and the correlation coefficients (R^2) were very low. So the adsorption kinetics was not described by pseudo-first-order. On the other side, it indicated that pseudo-second-order model described the experimental data well. It was demonstrated by correlation coefficients (R^2) that were close to 1 as well as the theoretical values of q_e for the two heavy metal ions close to the experimental q_e values. This suggests that

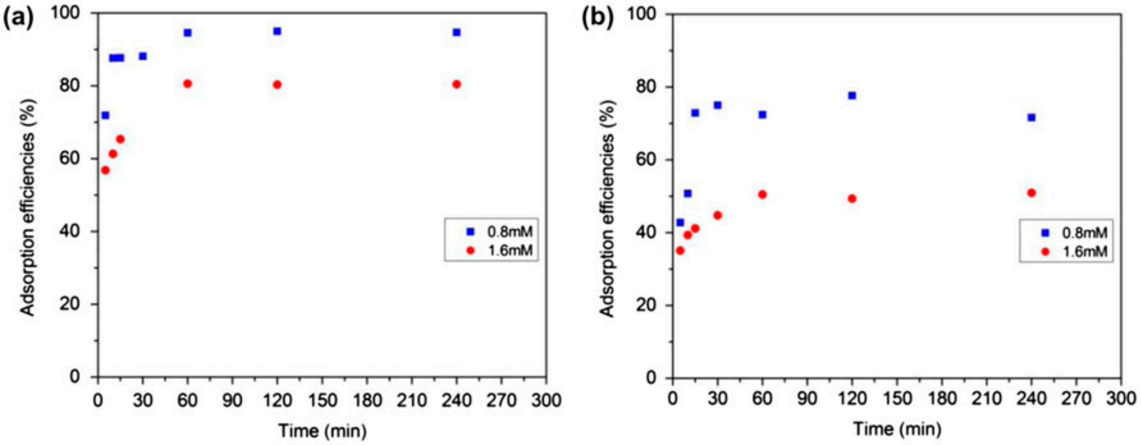

Fig. 7. Effect of contact time on the adsorption of Cd (a) and Ni (b) onto zeolite (pH 4.5, initial concentration 0.8 and 1.6 mM, respectively).

Table 3
The parameters of pseudo-first-order, pseudo-second-order, and Bangham equations

			Pseudo-second-order			Pseudo-first-order			Bangham equation		
Metal ions	Initial concentration (mmol/L)	$q_{e,exp}$ (mmol/g)	$q_{e,cal}$ (mmol/g)	K_2 (g/mmol h)	R^2	$q_{e,cal}$ (mmol/g)	K_1 (g/mmol h)	R^2	m	K_b (mmol/g)	R^2
Cd	0.8	0.08	0.08	9.89	1	0.008	0.014	0.63	15.67	0.06	0.65
	1.6	0.13	0.13	2.83	1	0.02	0.017	0.69	9.80	0.08	0.92
Ni	0.8	0.06	0.06	21.23	0.99	0.008	0.005	0.16	9.10	0.05	0.71
	1.6	0.08	0.08	2.56	1	0.023	0.015	0.60	5.62	0.03	0.93

chemisorption process could be a rate limiting step [27].

Besides, the kinetic curve could be divided into two portions and described well by intraparticle diffusion model, which indicated that the intraparticle diffusion was one of the limiting steps for Cd and Ni adsorption by zeolite:

$$q_t = k_i t^{0.5} + C \tag{11}$$

where k_i is the intraparticle diffusion constant (mmol/g min$^{0.5}$). This can be obtained from plot of q_t vs. $t^{0.5}$. C is a non-zero value revealing that the adsorption process is not controlled only by intraparticle diffusion but involves other adsorption steps occurring in this adsorption process (e.g. ion exchange, chemisorption process of silanol and aluminol groups, and main physisorption process).

3.5. The effect of temperature

Increasing temperature can increase the rate of diffusion of metal ions across the external boundary layer and in the internal pores of the adsorbent particle [28]. In addition, changing temperature alters the equilibrium capacity of the adsorbent [29]. Fig. 8 shows the effect of temperature on the adsorption of Cd and Ni onto zeolite. It showed that the adsorption efficiency increased from 95.6 to 98.5% when the temperature increased from 18 to 45℃. The increase of adsorption capacity with temperature increasing indicates the endothermic nature of Cd and Ni onto zeolite [30].

3.6. Adsorption mechanism

3.6.1. Ion-exchange mechanism

Zeolites are micro-porous crystalline, hydrated aluminosilicates that can be considered as inorganic polymers built from an infinitely extending three-dimensional network of tetrahedral SiO_4 and AlO_4 units which contain interconnected tunnels and voids. During the ion-exchange process, metal ions can move into the pores, channels, or voids of the lattice, and they can replace exchangeable cations (mainly Na^+) [31].

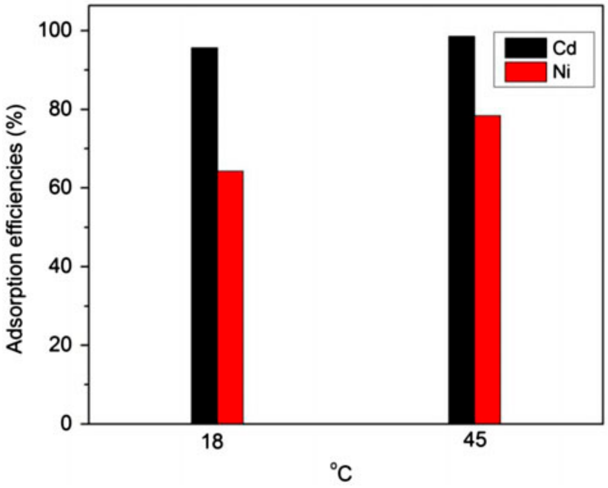

Fig. 8. Effect of temperature on adsorption efficiency of Cd and Ni onto zeolite.

In this study, ion exchange could be one of the primary mechanisms for metal ions removal as the zeolite exhibited high CEC. The values for net release of Na^+ (meq/g) due to Cd and Ni adsorption are presented in Table 4. The results showed a significant release of Na^+ from zeolite due to the adsorption of Cd and Ni. It was observed that 0.30 meq/g of Cd and 0.29 meq/g of Ni were adsorbed onto zeolite, meanwhile 0.36 meq/g Na^+ was released. This would mean that cation exchange (exchangeable Na^+ present in zeolite) involved in the adsorption of Cd and Ni ions onto zeolite, which suggested that ion exchange was one of the primary adsorption mechanism. The ion-exchange reaction is represented as follows:

$$\text{Zeolite} - 2Na^+ + M^{2+} \longrightarrow 2Na^+ + \text{Zeolite} - M^{2+} \tag{12}$$

Meanwhile, it was observed that net amount of Na^+ released (0.36 meq/g) was less than total metal ions adsorbed (0.30 meq/g of Cd and 0.29 meq/g of Ni), which suggested other adsorption mechanism as supplementary could occur in the adsorption process.

Table 4
Release amount of Na^+ due to adsorption of Cd and Ni onto zeolite

Metal ions	Total metal ions adsorbed (meq/g)	Net amount of Na^+ released (meq/g)
Cd	0.30	0.36
Ni	0.29	

3.6.2. Other adsorption mechanism

The other adsorption mechanisms of zeolite for Cd and Ni were also proposed as follows:

(1) Electrostatic attraction. The equilibrium pH in adsorption experiment was generally greater than the pH_{pzc} of zeolite. Therefore, the surface or at least part of the surface of zeolite carried negative charge. The species of Cd and Ni ion carrying positive charge, i.e. Cd^{2+}, Ni^{2+} and $CdOH^+$, $NiOH^+$, should be attracted to the surface of zeolite [32].

(2) Surface complex formation. The hydrous silicon oxide and aluminum oxide in the surface of zeolite makes that oxide surface has high affinity toward metal ions. It can complex with metal ions by chemical bonding [33]. The type of complex formation includes monodentate and bidentate types [34]. Hydrous oxides in the surface can form complex with metal ions by chemical bonding, which allows that metals (M^{2+}) make complex at the surface (Eqs. (13)–(16)):

$$2(\equiv SiO^-) + M^{2+} \longrightarrow (\equiv SiO)_2 M \tag{13}$$

$$2(\equiv AlO^-) + M^{2+} \longrightarrow (\equiv AlO)_2 M \tag{14}$$

$$\equiv Si\text{-}O^- + M^{2+} \longrightarrow \equiv Si\text{-}O^- M^{2+} \tag{15}$$

$$\equiv Al\text{-}O^- + M^{2+} \longrightarrow \equiv Al\text{-}O^- M^{2+} \tag{16}$$

3.7. FTIR and Energy-dispersive X-ray analysis

FTIR analysis was used to identify some characteristic functional groups and the spectra of zeolite before and after metal ions adsorption are shown in Fig. 9. The FTIR spectrum of original zeolite shows a strong broad band at 3,460 cm^{-1} which indicates the presence of hydroxyl groups on zeolite. The band appearing at 980 cm^{-1} can be attributed to zeolite tetrahedral SiO_4 and AlO_4 of asymmetric stretching vibrations. The band at 459 cm^{-1} is attributed to the flexure vibration of Si(Al)–O; bands at 748 and 702 cm^{-1} are due to the symmetry stretching vibration of Si(Al)–O–Si [34]. All these bands of zeolite after metal ions adsorption were shifted significantly, such as the band at 980 cm^{-1} was shifted to 1,100 cm^{-1} after adsorption, suggesting the adsorption of Cd and Ni on the active sites of Si(Al)–O bond.

The energy-dispersive X-ray (EDS) patterns of zeolite before and after the adsorption of Cd and Ni are shown in Fig. 10. The EDS pattern for the unloaded

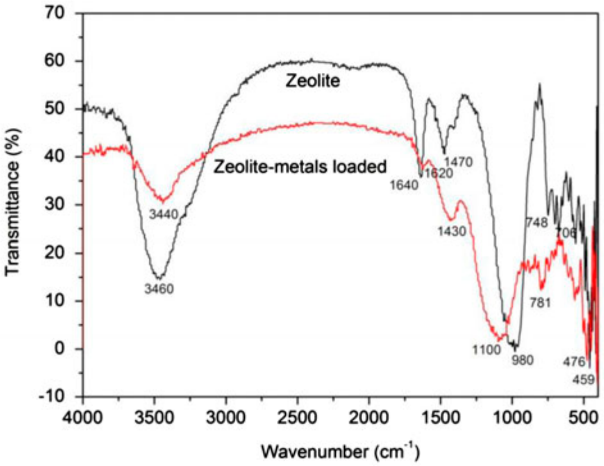

Fig. 9. FTIR spectra of zeolite before and after metals adsorption.

zeolite did not show the characteristic signal of Cd and Ni (Fig. 10(a)), whereas clear signals of the presence of Cd and Ni were observed for the Cd- and Ni-loaded zeolite (Fig. 10(b)), which provided a direct evidence for Cd and Ni adsorption on the surface of zeolite.

4. Conclusion

In this study, the synthetic zeolite X (octahedral crystal) was produced from CBA using alkaline fusion method and applied to remove Cd and Ni from acidic wastewater. The result suggested that the synthetic zeolite was an excellent adsorbent for metals removal, because of the characteristics of high specific surface area, specific pore volume, and CEC. The adsorption isotherms can be well described by the Langmuir, Freundlich, and DKR models, and the maximum

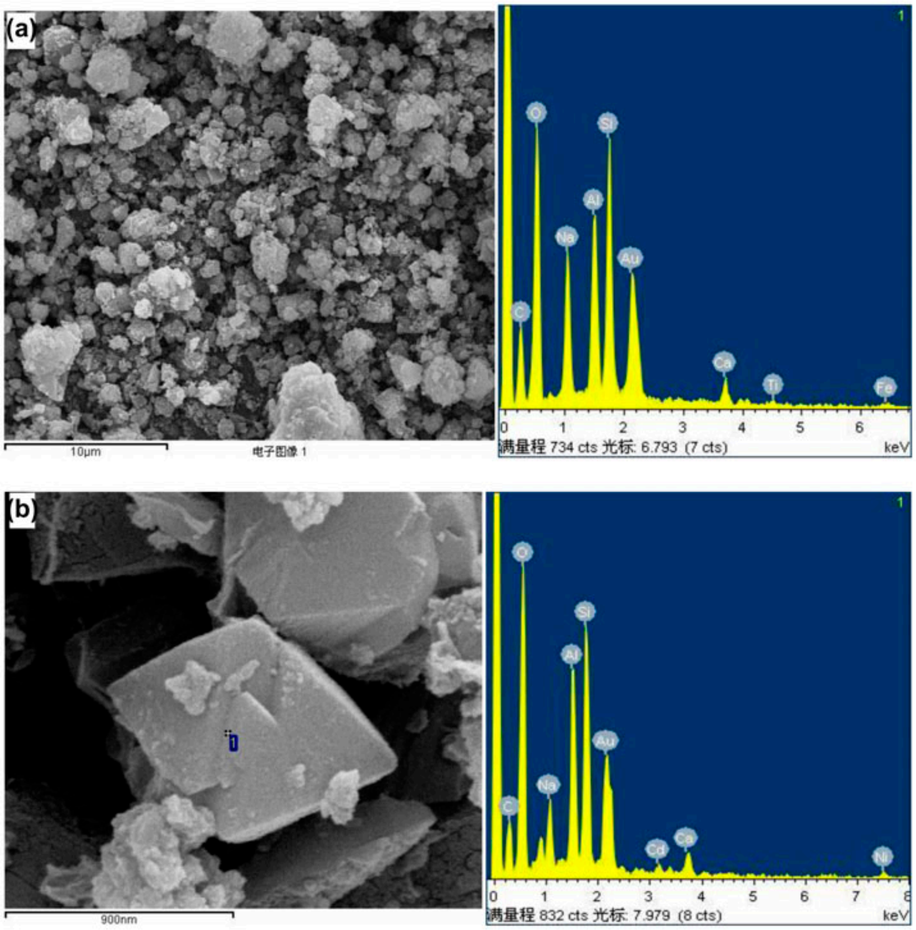

Fig. 10. EDS analysis of zeolite before (a) and after (b) the adsorption of Cd and Ni.

adsorption capacity of Cd and Ni onto zeolite was 1.18 and 1.35 mmol/g, respectively. Compared with single-solute system, in the multiple-solute system the adsorption capacity for Cd or Ni decreased to 1.04 and 0.92 mmol/g, respectively, due to the competition effect. The solution pH was the key factor affecting the adsorption efficiency and the adsorption equilibrium was achieved at around 5.5 (>pH_{pzc} 4.5). Kinetic data showed that the adsorption process achieved equilibrium within 4 h and followed the pseudo-second-order model well. Ion exchange was found to be the primary adsorption mechanism, supplemented by complexation by Si(Al)–O group, and electrostatic attraction.

Acknowledgments

This work was supported by Water Conservancy Research and Technology Promotion Project of Shandong Province [SDSLKY201306] (Key technology research and demonstration of saline water sub-desalination in the Yellow River Delta), the National Natural Science Foundation of China [51204075] and Shandong Provincial Key Research and Development Program [2015GSF117014].

References

[1] G.Z. Kyzas, N.K. Lazaridis, M. Kostoglou, On the simultaneous adsorption of a reactive dye and hexavalent chromium from aqueous solutions onto grafted chitosan, J. Colloid Interface Sci. 407 (2013) 432–441.

[2] A. Mittal, J. Mittal, A. Malviya, V.K. Gupta, Removal and recovery of Chrysoidine Y from aqueous solutions by waste materials, J. Colloid Interface Sci. 344 (2010) 497–507.

[3] M.E. Lee, J.H. Park, J.W. Chung, C.Y. Lee, S. Kang, Removal of Pb and Cu ions from aqueous solution by Mn_3O_4-coated activated carbon, J. Ind. Eng. Chem. 21 (2015) 470–475.

[4] V.K. Gupta, S. Agarwal, T.A. Saleh, Synthesis and characterization of alumina-coated carbon nanotubes and their application for lead removal, J. Hazard. Mater. 185 (2011) 17–23.

[5] N. Koukouzas, C. Ketikidis, G. Itskos, Heavy metal characterization of CFB-derived coal fly ash, Fuel Process. Technol. 92 (2011) 441–446.

[6] L.C. Ram, R.E. Masto, An appraisal of the potential use of fly ash for reclaiming coal mine spoil, J. Environ. Manage. 91 (2010) 603–617.

[7] S. Wang, Z.H. Zhu, Effects of acidic treatment of activated carbons on dye adsorption, Dyes Pigm. 75 (2007) 306–314.

[8] M.R. Malekbala, M.A. Khan, S. Hosseini, L.C. Abdullah, T.S. Choong, Adsorption/desorption of cationic dye on surfactant modified mesoporous carbon coated monolith: Equilibrium, kinetic and thermodynamic studies, J. Ind. Eng. Chem. 21 (2015) 369–377.

[9] V.K. Gupta, A. Mittal, L. Krishnan, J. Mittal, Adsorption treatment and recovery of the hazardous dye, Brilliant Blue FCF, over bottom ash and de-oiled soya, J. Colloid Interface Sci. 293 (2006) 16–26.

[10] S. Mohan, R. Gandhimathi, Removal of heavy metal ions from municipal solid waste leachate using coal fly ash as an adsorbent, J. Hazard. Mater. 169 (2009) 351–359.

[11] M. Zhang, H. Zhang, D. Xu, L. Han, D. Niu, L. Zhang, W. Wu, B. Tian, Ammonium removal from aqueous solution by zeolites synthesized from low-calcium and high-calcium fly ashes, Desalination 277 (2011) 46–53.

[12] A.M. Cardoso, A. Paprocki, L.S. Ferret, C.M. Azevedo, M. Pires, Synthesis of zeolite Na-P1 under mild conditions using Brazilian coal fly ash and its application in wastewater treatment, Fuel 139 (2015) 59–67.

[13] E. Erdem, N. Karapinar, R. Donat, The removal of heavy metal cations by natural zeolites, J. Colloid Interface Sci. 280 (2004) 309–314.

[14] R. Apiratikul, P. Pavasant, Sorption of Cu^{2+}, Cd^{2+}, and Pb^{2+} using modified zeolite from coal fly ash, Chem. Eng. J. 144 (2008) 245–258.

[15] C. Belviso, E. Agostinelli, S. Belviso, F. Cavalcante, S. Pascucci, D. Peddis, G. Varvaro, S. Fiore, Synthesis of magnetic zeolite at low temperature using a waste material mixture: Fly ash and red mud, Microporous Mesoporous Mater. 202 (2015) 208–216.

[16] N. Koukouzas, C. Vasilatos, G. Itskos, I. Mitsis, A. Moutsatsou, Removal of heavy metals from wastewater using CFB-coal fly ash zeolitic materials, J. Hazard. Mater. 173 (2010) 581–588.

[17] N. Murayama, H. Yamamoto, J. Shibata, Mechanism of zeolite synthesis from coal fly ash by alkali hydrothermal reaction, Int. J. Miner. Process. 64 (2002) 1–17.

[18] X. Querol, N. Moreno, J.C. Umaña, A. Alastuey, E. Hernández, A. López-Soler, F. Plana, Synthesis of zeolites from coal fly ash: An overview, Int. J. Coal Geol. 50 (2002) 413–423.

[19] Available from: <http://www.epa.gov/epaoswer/hazwaste/test/pdfs/9081.pdf>.

[20] H. Chen, J. Zhao, J. Wu, G. Dai, Isotherm, thermodynamic, kinetics and adsorption mechanism studies of methyl orange by surfactant modified silkworm exuviae, J. Hazard. Mater. 192 (2011) 246–254.

[21] F.H. Frimmel, L. Huber, Influence of humic substances on the aquatic adsorption of heavy metals on defined mineral phases, Environ. Int. 22 (1996) 507–517.

[22] M.S. Mansour, M.E. Ossman, H.A. Farag, Removal of Cd (II) ion from waste water by adsorption onto polyaniline coated on sawdust, Desalination 272 (2011) 301–305.

[23] F. Qin, B. Wen, X.Q. Shan, Y.N. Xie, T. Liu, S.Z. Zhang, S.U. Khan, Mechanisms of competitive adsorption of Pb, Cu, and Cd on peat, Environ. Pollut. 144 (2006) 669–680.

[24] P. Ricou, I. Lecuyer, P. Le Cloirec, Influence of pH on removal of heavy metallic cations by fly ash in aqueous solution, Environ. Technol. 19 (1998) 1005–1016.

[25] C.A.P. Almeida, N.A. Debacher, A.J. Downs, L. Cottet, C.A.D. Mello, Removal of methylene blue from colored effluents by adsorption on montmorillonite clay, J. Colloid Interface Sci. 332 (2009) 46–53.

[26] M.S. Rahman, M.R. Islam, Effects of pH on isotherms modeling for Cu(II) ions adsorption using maple wood sawdust, Chem. Eng. J. 149 (2009) 273–280.

[27] Y.S. Ho, G. McKay, Sorption of dye from aqueous solution by peat, Chem. Eng. J. 70 (1998) 115–124.

[28] K.J. Wang, B.S. Xing, Mutual effects of cadmium and phosphate on their adsorption and desorption by goethite, Environ. Pollut. 127 (2004) 13–20.

[29] M. Visa, C. Bogatu, A. Duta, Simultaneous adsorption of dyes and heavy metals from multicomponent solutions using fly ash, Appl. Surf. Sci. 256 (2010) 5486–5491.

[30] S. Chowdhury, R. Mishra, P. Saha, P. Kushwaha, Adsorption thermodynamics, kinetics and isosteric heat of adsorption of malachite green onto chemically modified rice husk, Desalination 265 (2011) 159–168.

[31] T. Hsu, C. Yu, C. Yeh, Adsorption of Cu^{2+} from water using raw and modified coal fly ashes, Fuel 87 (2008) 1355–1359.

[32] C.P. Huang, E.A. Rhoads, Adsorption of Zn(II) onto hydrous aluminosilicates, J. Colloid Interface Sci. 131 (1989) 289–306.

[33] S.C. Pan, C.C. Lin, D.H. Tseng, Reusing sewage sludge ash as adsorbent for copper removal from wastewater, Resour. Conserv. Recycl. 39 (2003) 79–90.

[34] Y. Zhang, L. Jing, X. He, Y. Li, X. Ma, Sorption enhancement of TBBPA from water by fly ash-supported nanostructured γ-MnO_2, J. Ind. Eng. Chem. 21 (2015) 610–619.